Fluorobenzene−Nucleobase Interactions: Hydrogen Bonding or π-Stacking?

Roman Leist, Jann A. Frey, and Samuel Leutwyler*

Departement für Chemie und Biochemie, Universität Bern, Freiestrasse 3, CH-3012 Bern, Switzerland

Received: December 6, 2005; In Final Form: February 2, 2006

Studies on modified DNA oligomers and polymerase reactions have previously demonstrated that canonical nucleobases can exhibit stable and even selective pairing with shape-complementary fluorobenzene nucleotides. Because of the fluorination of the pairing edges, hydrogen bonds are believed to be absent, and the local DNA stability has been attributed to π-stacking and shape complementarity. Using two-color resonant two-photon ionization and fluorescence emission spectroscopies, we show here that supersonically cooled complexes of the nucleobase analogue 2-pyridone with seven substituted fluorobenzenes (1-fluorobenzene, 1,2- and 1,4-difluorobenzene, 1,3,5- and 1,2,3-trifluorobenzene, 1,2,4,5- and 1,2,3,4-tetrafluorobenzene) are hydrogen-bonded and not π-stacked. The $S_1 \leftrightarrow S_0$ vibronic spectra show intermolecular vibrational frequencies that are characteristic for doubly hydrogen bonded complexes. The 0_0^0 bands shift to the blue with increasing hydrogen-bond strength; the measured spectral blue shifts $\delta\nu$ are in excellent agreement with the ab initio calculated shifts. The spectral shifts are also linearly correlated with the calculated hydrogen-bond dissociation energies D_0, published in a companion paper (Frey, J. A.; Leist, R.; Leutwyler, S. *J. Phys. Chem. A* **2006**, *110,* 4188). This correlation allows us to reliably estimate the ground-state dissociation energies as $D_0 \approx$ 6 kcal/mol of the 2-pyridone·fluorobenzene complexes from the observed spectral shifts.

I. Introduction

The biological storage and transmission of genetic information is based on size complementarity (purine/pyrimidine pairing) and the complementary Watson−Crick hydrogen-bonding patterns of the base pairs in double-stranded DNA, mRNA, and tRNA. Regarding the role of the Watson−Crick hydrogen-bonding for DNA and RNA polymerase transcription fidelity, a number of studies with modified DNA oligomers have shown stable—and in several cases even selective—base pairing using nonpolar nucleobase analogues whose pairing edges are partly or wholly fluorinated.[1−10] In these analogues, the N−H or C═O hydrogen-bonding functional groups have been replaced by nominally non-hydrogen-bonding groups such as C−H or C−F. The base pair stability and polymerase selectivity have been interpreted in terms of base stacking, hydrophobic, and "shape complementarity" effects.[1−10]

In the fields of supramolecular synthesis and crystal engineering, the existence and strengths of weak C−F···H−X (X = C, N, O) hydrogen bonds has been investigated via the analysis of data collected in the Cambridge Crystallographic Structural Database. Crystallographic evidence of C−F···H−X (X = C, N, O) hydrogen bonds had first been reported by Glusker and Shimoni.[11] The evidence from crystal structures seems to show that C−F bonds are at best weak hydrogen bond acceptors and C−F···H−X hydrogen bonds are observed only in absence of a better acceptor,[11−13] or as Dunitz has put it: "Organic fluorine hardly ever makes hydrogen bonds".[13] The above conclusions have typically been determined on complex systems at room temperature in which crystal packing effects, solvation/desolvation properties, and entropic contributions play a considerable role. However, little detailed understanding of the underlying intermolecular interactions is forthcoming from these studies. Specifically, it remains unclear whether hydrogen bonds to C−F groups are indeed absent, especially in the case of fluorinated base pair moieties.

Here, we investigate the extent of (or absence of) hydrogen bonding in complexes formed between the nucleobase analogue 2-pyridone (2PY) and seven different fluorobenzenes in supersonic beams. The supersonic jet temperatures are close to 0 K, and solvation and crystal packing effects, DNA backbone constraints, ionic effects, and entropic contributions are nonexistent. Complexes of 2PY with fluorobenzene (1-FB), 1,2-difluorobenzene (1,2-FB), 1,4-difluorobenzene (1,4-FB), 1, 2, 3-trifluorobenzene (1,2,3-FB), 1,3,5-trifluorobenzene (1,3,5-FB), 1,2,4,5-tetrafluorobenzene (1,2,4,5-FB), and 1,2,3,4-tetrafluorobenzene (1,2,3,4-FB) were investigated using mass-specific laser spectroscopic techniques.

2-Pyridone (2PY) can be viewed as the simplest possible hydrogen-bonding analogue of uracil and thymine. Indeed, Yokoyama and co-workers have recently synthesized nucleosides with 2PY as a substitute for thymine and find it to be enzymatically replicable when paired with 2-amino-6-(2-thienyl) purine.[14−16] In addition, the 2-pyridone nucleoside is strongly fluorescent and enables the site-specific fluorescent labeling of RNA molecules.[17] A number of hydrogen-bonded complexes of 2PY with H-donors, H-acceptors, and nucleobases have been recently studied by supersonic-jet spectroscopy.[18−23] We have found that the spectral shift of the 2PY $S_1 \leftrightarrow S_0$ electronic origin is a sensitive function of the N−H···X and X···O═C hydrogen-bond strengths of the hydrogen bond(s) over a large range of H-bonding strengths.[22]

We show below that all seven 2-pyridone·fluorobenzene complexes are doubly hydrogen bonded, as diagnosed by the electronic spectral shifts and the inter- and intramolecular vibrational frequencies. Figure 1 shows these hydrogen-bonded 2PY·fluorobenzene geometries. We have not been able to find any experimental evidence for π-stacked complexes between

10.1021/jp057100h CCC: $33.50
Published on Web 03/04/2006

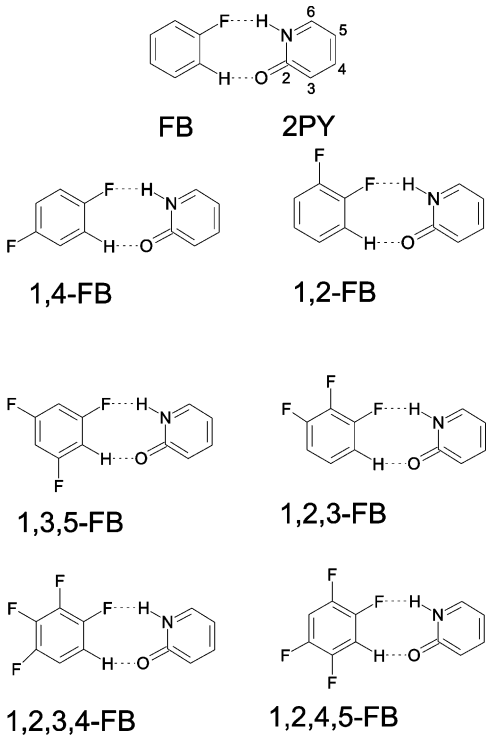

Figure 1. Structures of the 2-pyridone·fluorobenzene complexes. The abbreviations of the respective fluorobenzene moieties and atom numbering of the 2-pyridone moiety are indicated.

2PY and the fluorobenzenes with one to four F atoms. The experimental data is in excellent agreement with ab initio calculations presented in a companion paper.[24] These predict that the most stable 2-pyridone−fluorobenzene dimers are bound via neighboring N−H···F−C and C−H···O═C hydrogen bonds.

II. Experimental Methods

The 2PY·fluorobenzene complexes were synthesized and cooled in a 20-Hz pulsed supersonic expansion through a thin-walled 0.6-mm-diameter nozzle, using Ne carrier gas at a backing pressure of 0.9−1.2 bar. The Ne carrier gas was flowed through a stainless steel tube cooled to about −35 °C that contained the fluorobenzene (1-FB, 1,2-FB, and 1,4-FB Fluka ∼98%; 1,3,5-FB Fluka ≥98%; 1,2,4,5-FB Aldrich 99%). 2-Pyridone (Aldrich, 97%) was placed in the nozzle and heated to 85−90 °C. Mass-selected two-color resonant two-photon ionization (2C−R2PI) spectra were measured in the region 29 850−31 000 cm^{-1} by crossing the skimmed supersonic jet with the unfocused UV excitation and ionization laser beams that were brought to spatial and temporal overlap in the source of a linear time-of-flight mass spectrometer. $S_1 \leftarrow S_0$ excitation was performed by a frequency-doubled dye laser at pulse energies of 0.2−1 mJ, pumped by the second harmonic of a Nd:YAG laser. For ionization, the fourth harmonic (266 nm) of the same Nd:YAG laser was used at energies of 2−3 mJ/pulse. The ions were detected using double multichannel plates. The resulting mass spectra were digitized in a LeCroy LT374 digitizer, averaged over 64 laser shots, and transferred to a PC.

For the dispersed fluorescence experiments, the UV laser beam crossed the jet at ∼2 mm from the nozzle. The emitted fluorescence was collected using a combination of spherical mirror and quartz optics and dispersed with a SOPRA F1500 UHRS 1.5 m monochromator. The dispersed fluorescence light was detected by a cooled Hamamatsu R928 photomultiplier and averaged over 64 or 128 laser shots.

TABLE 1: Selected Pyramidalization Dihedral Angles τ (deg) of 2-Pyridone in the S_1 Excited State from CIS/6-31G(d,p) Calculations[a]

molecule	τ(H−N−C_2−C_6)	τ(H−N−C_6−C_5)	τ(N−C_2−C_6−C_5)
2PY·FB	30.1	5.6	20.9
2PY·1,2-FB	31.1	5.9	21.5
2PY·1,4-FB	30.8	5.7	21.4
2PY·1,2,3-FB	32.0	6.0	22.2
2PY·1,3,5-FB	32.3	6.1	22.4
2PY·1,2,4,5-FB	32.7	6.1	23.0
2PY·1,2,3,4-FB	33.2	6.3	22.7

[a] For atom numbering, refer to Figure 1.

III. Results and Discussion

A. S_1 State ab Initio Calculations. The minimum-energy structures and harmonic vibrational frequencies of the S_1 excited state were calculated using the configuration interaction singles (CIS) method with the 6-31G(d,p) basis set, using *Gaussian 03*.[25] The S_1 geometry of all complexes is predicted to be nonplanar. The 2PY moiety, which is planar in the S_0 ground state, is pyramidalized at the N−H group upon $S_1 \leftarrow S_0$ excitation, leading to two equivalent out-of-plane minima. We characterize this distortion by the dihedral angles τ(H−N−C_2−C_6) and τ(H−N−C_6−C_5); the atom numbering is indicated in Figure 1. These angles are in the ranges 30−33°, and 5.5−6.5°; see also Table 1. The excited-state distortion of 2PY is also characterized by a "flap" distortion of the 2PY ring, expressed by the angle τ(N−C_2−C_6−C_5), which is in the range 21−23°; see Table 1. On the other hand, the carbonyl group remains nearly coplanar with the rest of the ring, since the calculated dihedral angle τ(O═C_2−N−C_3) is <0.7° for all complexes. The excited-state pyramidalization at the N atom is spectroscopically observed as vibronic excitations of the intramolecular out-of-plane modes ν'_1 and ν'_2 of 2PY, as discussed below.

The calculated CIS/6-31G(d,p) intermolecular and selected intramolecular vibrational wavenumbers are compiled in Table 2. The intermolecular vibrational wavenumbers depend on the force fields of the two hydrogen bonds and the mass distributions of the two monomer moieties. They differ by up to 15%, depending on the specific fluorobenzene partner and are characteristic for each complex.

B. Two-Color Resonant Two-Photon Ionization (R2PI) spectra. The $S_1 \leftarrow S_0$ spectra of 2PY·FB, 2PY·1,4-FB, 2PY·1,2-FB, 2PY·1,3,5-FB, and 2PY·1,2,3-FB were measured by the two-color R2PI technique and are shown in Figure 2(a−e). The ionization potentials of the 2PY·1,2,3,4-FB and 2PY·1,2,4,5-FB complexes are slightly higher than those of the other five complexes, and ionization could not be achieved at 266 nm. These two spectra are measured by laser-induced fluorescence and are shown in Figure 2f,g.

The concentrations of the different 2PY·fluorobenzene dimers in the supersonic beam are relatively low, since their formation is in competition with that of the much more strongly bound (2-pyridone)$_2$ self-dimer, which has a calculated $D_0 = -20.8$ kcal/mol.[23,26] The relative concentration was measured for 2PY·FB, which has the same mass as the ^{13}C isotopomer of (2-pyridone)$_2$. The electronic origin band of the latter (which is present at 11.0% of the total (2PY)$_2$ signal) is twice that of the electronic origin of 2PY·FB.

The lowest-wavenumber and most intense band of each R2PI spectrum in Figure 2 is assigned as the $S_1 \leftarrow S_0$ electronic origin. The lowest-wavenumber origin of the entire series is that of

TABLE 2: Calculated S_1 State Vibrational Wavenumbers (in cm^{-1}) of the 2-Pyridone·Fluorobenzene Complexes at the CIS/6-31G(d,p) Level

	2PY·FB	2PY·1,4-FB	2PY·1,2-FB	2PY·1,2,3-FB	2PY·1,3,5-FB	2PY·1,2,3,4-FB	2PY·1,2,4,5-FB
buckle β'	7.2	7.0	7.8	7.5	6.7	7.4	7.4
twist θ'	33.2	33.3	28.6	26.4	23.4	26.5	24.3
stagger δ'	36.4	35.9	34.4	31.9	32.8	31.4	31.4
opening ω'	47.1	44.6	46.7	43.6	42.4	41.6	41.6
shear χ'	53.6	51.2	51.9	49.9	47.6	48.2	47.6
stretch σ'	73.9	73.3	67.5	65.5	67.1	67.1	68.4
			2-Pyridone Monomer Intramolecular Vibrations				
N−H oop ν_1'	103.8	105.5	106.4	108.7	108.9	110.5	111.4
ν_2'	230.1	231.0	231.4	232.4	232.2	233.5	233.8
ν_3'	415.1	413.5	413.6	412.5	413.5	411.4	412.4
ν_4'	485.8	483.7	485.3	484.7	484.7	484.4	484.5
ν_5'	565.2	563.8	563.3	561.9	561.3	560.9	560.2
ν_6'	585.4	585.0	584.3	583.3	583.1	583.2	583.4
ν_7'	617.2	618.1	617.7	616.9	617.5	618.2	620.2
ν_8'	664.8	664.9	664.6	664.6	664.6	664.8	664.8
ν_{11}'	833	832	830	831.4	830	831.1	831

2PY·FB at 30 038.1 cm^{-1}. As Figure 2 shows, the origins shift systematically to higher energies with increasing degree of fluorination, by ~60 cm^{-1} for the difluorobenzenes, by 70 and 80 cm^{-1} for the trifluorobenzenes, and by 140−150 cm^{-1} for the tetrafluorobenzenes. The spectral shift behavior will be discussed below.

At wavenumbers of <100 cm^{-1}, the most prominent bands are due to the three in-plane intermolecular vibrations: These

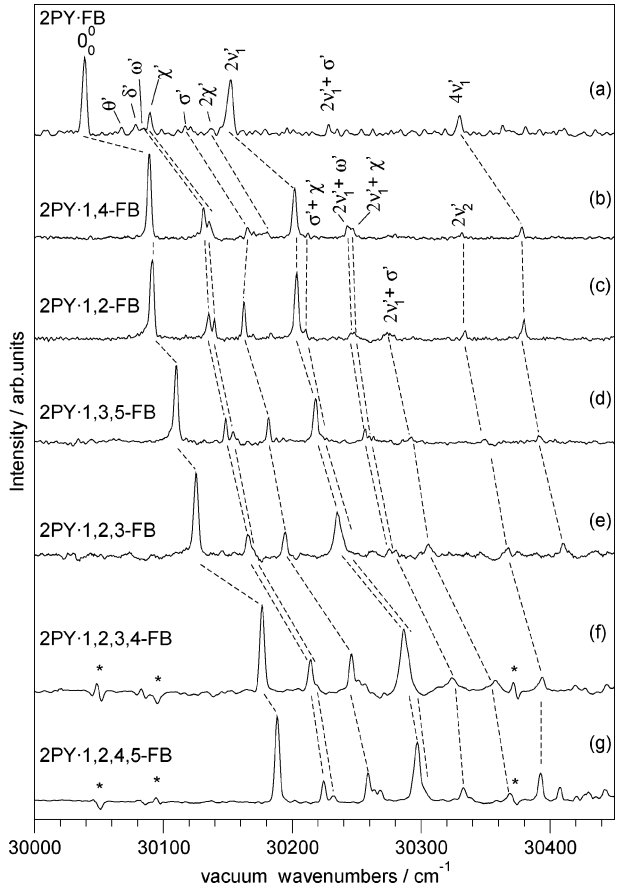

Figure 2. Two-color resonant two-photon ionization spectra of (a) 2-pyridone·fluorobenzene, (b) 2-pyridone·1,4-difluorobenzene, (c) 2-pyridone·1,2-difluorobenzene, (d) 2-pyridone·1,3,5-trifluorobenzene, and (e) 2-pyridone·1,2,3-trifluorobenzene. Laser-induced fluorescence spectra are shown for (f) 2-pyridone·1,2,3,4-tetrafluorobenzene and (g) 2-pyridone·1,2,4,5-tetrafluorobenzene. The respective spectral contributions of 2-pyridone to spectra (f) and (g) have been subtracted; asterisks indicate slight artifacts from the subtraction procedure.

are the opening mode ω', the shear mode χ', and the stretching mode σ'. We discuss these excitations for the two-color R2PI spectrum of 2PY·1,2-FB, shown in Figure 2c, where all three excitations are relatively strong and clearly resolved. The $S_1 \leftarrow S_0$ origin lies at 30 091.4 cm^{-1}. The close-lying bands at 43.8 and 48.3 cm^{-1} can be identified as the in-plane intermolecular opening ω' and shear χ' vibrations, based on the CIS/6-31G(d,p) wavenumbers of 46.7 and 51.9 cm^{-1}; see Table 2. The intense band at 71 cm^{-1} is assigned to the stretching mode σ'; this is in good agreement with the CIS/6-31G(d,p) value of 67.5 cm^{-1}.

A similar intensity pattern of the ω', χ', and σ' excitations is observed in the 2C−R2PI spectrum of 2PY·1,3,5-FB, shown in Figure 2d; however, the Franck−Condon factor of the χ' excitation is weaker than for 2PY·1,2-FB. Analogous intermolecular vibrational patterns for ω', χ', and σ' are observed for the complexes 2PY·1,2,3-FB, 2PY·1,2,3,4-FB, and 2PY·1,2,3,5-FB, shown in Figure 2e,f,g, respectively. Throughout this series, the ω' and σ' bands have comparable Franck−Condon factors, while the χ' excitation, observed on the high-energy side of the ω' band, is about three times weaker. In contrast, the σ' excitation in the R2PI spectrum of 2PY·1,4-FB, shown in Figure 2b, is much weaker than the ω' band. For 2PY·fluorobenzene, the σ' band at 65 cm^{-1} is very weak. The S_1 state vibrational wavenumbers and their assignments are given in Tables 3−5.

Figure 3 compares the calculated CIS harmonic intermolecular vibrational wavenumbers to experiment. Generally, the ω' and χ' wavenumbers are predicted slightly too low and the σ' wavenumbers slightly too high, but the differences are small, typically <3 cm^{-1}. The overall trends of the three wavenumbers as a function of degree of fluorination are completely consistent with experiment.

C. S_1 State Intramolecular Excitations of 2-Pyridone. At higher wavenumbers, several intramolecular excitations of the 2PY moiety are identified in the spectra of the complexes. The $S_1 \leftarrow S_0$ spectrum of jet-cooled 2-pyridone has been measured by resonance-enhanced multiphoton ionization by Nimlos et al.[27] and by Kimura et al.[28] The spectrum breaks off ~500 cm^{-1} above the origin, the vibronic band structure is irregular, and no definite S_1 state vibronic assignments have been given so far. The two strongest bands at 29 831 and 29 930 cm^{-1} were assigned as two separate $S_1 \leftarrow S_0$ transitions ("A" and "B") originating from different ground states.[27] Later, Held and Pratt found that these two bands originate from the same ground-state level and correspond to two S_1 state conformers that differ in the degree of nonplanarity at the nitrogen atom.[29] This is in

TABLE 3: Experimental S_1 State Vibrational Wavenumbers of the 2-Pyridone·Fluorobenzene Complexes from Two-Color Resonant Two-Photon Ionization and LIF Spectra (see text)[a]

	2PY·1-FB	2PY·1,4-FB	2PY·1,2-FB	2PY·1,3,5-FB	2PY·1,2,3-FB	2PY·1,2,3,4-FB	2PY·1,2,4,5-FB
0_0^0	30 038.1	30 089.1	30 191.4	30 109.9	30 125.4	30 176.5	30 188.5
ω'	45	42.2	43.8	38.5	40.0	37.9	35.9
χ'	51	46.3	48.3	44.3	44.4	47.2	43.5
σ'	77	76.1	71.2	71.8	69.1	69.4	70.5
$2\omega'$				77.8		80.3	80.2
$\omega' + \theta'$			78.3				
$\omega' + \chi'$		85.5	92.2	83.1			
$2\chi'$				88.9	80.8	74.8	75.8
$2\nu_1'$	112.8	112.6	112.1	108.0	109.7	110.2	109.0
$2\nu_1' + \omega'$	157.4	153.7	154	146.6			
$2\nu_1' + \chi'$	163.7	157.8	157	153.0	155.0	147.6	144.5
$2\nu_1' + \sigma'$	190	190.4	183	181.2	180.3	180.9	182.0
$2\nu_2'$		242.5	242.3	239.3	242	243	240
$4\nu_1'$	291	289	288	281	284	282	281
ν_4'	444.0	444.3	444.0	444.1	444.2	444	443
$\nu_4' + \omega'/\chi'$		∼485	∼487				
$\nu_4' + \sigma'$		520	515.1	515	513		
ν_5'	525.7	525.3	524.6	524.0	523.9	524	523
ν_6'	548.7	549.0	548.0/550.	547.3	548.1	548	546

[a] All values in cm^{-1}, relative to the electronic origin.

TABLE 4: Experimental S_0 State Vibrational Wavenumbers of the 2-Pyridone·Fluorobenzene Complexes from Fluorescence Spectra[a]

	2PY·FB	2PY·1,4-FB	2PY·1,2-FB	2PY·1,3,5-FB	2PY·1,2,3-FB	2PY·1,2,3,4-FB	2PY·1,2,4,5-FB
0_0^0 ($S_1 \leftarrow S_0$)	30 038.1	30 089.1	30 191.4	30 109.9	30 125.4	30 176.5	30 188.5
ω''	48	45	44	40	41	40	40
χ''	55	50	49	47	44	44	44
$2\delta''$	76	49	73				
σ''	80	85	78	78	76	79	79
$\sigma'' + \omega''$	85	131					
$2\sigma''$		161					
ν_3''(2PY)	456	458	454	454	455	456	457
ν_5''(2PY)	543	545	541	541	542	544	545
ν_5''(2PY) + χ''		593	574	574	576		
ν_5''(2PY) + ω''		597	585	585	582		
ν_6''(2PY)	607	609	606	607	607	608	610
			615		619		
ν_5''(2PY) + σ''			621				

[a] All values in cm^{-1}, relative to the electronic origin.

TABLE 5: Calculated S_0 State Intermolecular Vibrational Wavenumbers (in cm^{-1}) of the 2-Pyridone·Fluorobenzene Complexes[a]

	2PY·FB	2PY·1,4-FB	2PY·1,2-FB	2PY·1,2,3-FB	2PY·1,3,5-FB	2PY·1,2,3,4-FB	1,2,4,5-FB
buckle β''	13.0	12.7	14.0	13.0	12.1	13.0	13.0
twist θ''	40.4	38.0	33.6	31.1	27.5	28.2	28.5
stagger δ''	52.5	48.2	50.1	43.2	44.1	40.7	40.7
opening ω''	52.7	51.7	47.9	45.9	45.5	46.5	46.5
shear χ''	56.4	53.5	54.6	52.5	50.4	49.8	49.8
stretch σ''	81.1	81.9	76.0	75.1	78.0	80.1	80.1

[a] All calculations with the B3LYP density functional and the 6-311++G(d,p) basis set.

agreement with later infrared spectroscopic and population labeling measurements of Mikami and co-workers.[30,31]

We have recently measured the $S_1 \leftrightarrow S_0$ spectra of 2PY by fluorescence-dip spectroscopy,[32] which reveals many more S_1 state vibrational excitations than the R2PI or fluorescence excitation spectra. This has allowed the identification of the S_1 state overtone transitions of the lowest-wavenumber out-of-plane pyramidalization modes, $2\nu_1'$ and $2\nu_2'$, and of the in-plane fundamental modes ν_3', ν_5' and ν_6'. The strong $2\nu_1'$ excitation was previously attributed to the "B" origin;[27] details will be presented elsewhere.[32] In the 2PY·fluorobenzenes, the $2\nu_1'$ overtone of 2PY gives rise to an intense band at ∼110 cm^{-1}, about 10% higher than in bare 2-pyridone.

The appearance of the low-wavenumber out-of-plane overtone excitations $2\nu_1'$, $4\nu_1'$, and $2\nu_2'$ in the R2PI spectra implies that the S_1 state 2PY is nonplanar also in the H-bonded complexes. This is in agreement with the CIS S_1 state calculations presented in section III.A and Table 1. In contrast to the intermolecular vibrations, the frequencies of this and the other intramolecular excitations are practically independent of the fluorobenzene moiety and lie within 2 for all the 2PY·FB complexes. Thus, $2\nu_1'$ varies between 112.8 cm^{-1} for 2PY·FB to 109 cm^{-1} for 2PY·1,2,4,5-FB. Combinations of $2\nu_1'$ with the three in-plane intermolecular vibrations such as $2\nu_1' + \omega'$, $2\nu_1' + \chi'$, and $2\nu_1' + \sigma'$ are observed in the spectra of all seven complexes, as listed in Table 3.

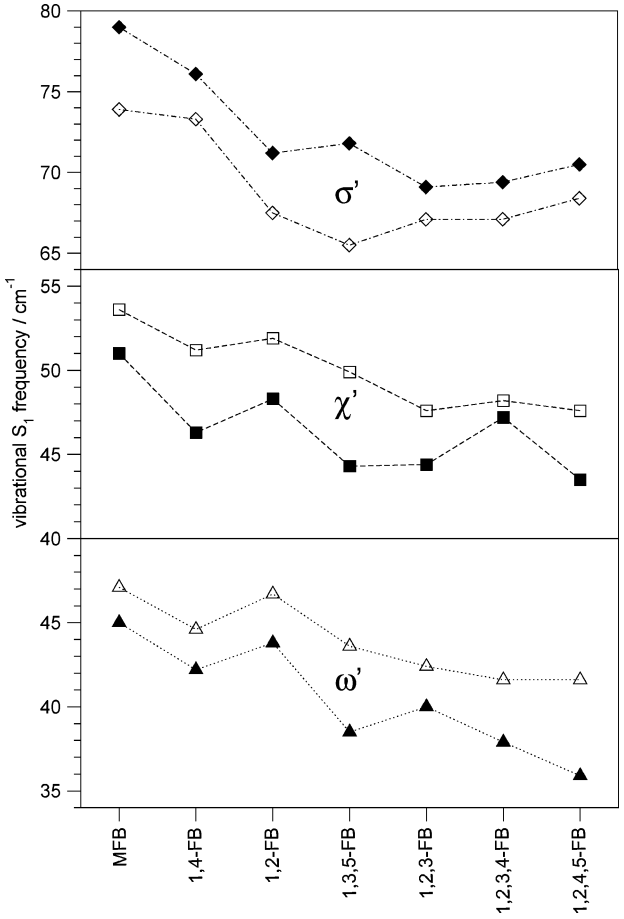

Figure 3. Comparison of the CIS/6-31G(d,p) calculated intermolecular S_1 state wavenumbers to experimental wavenumbers from the 2C−R2PI spectra. Filled symbols correspond to measured and empty symbols to calculated values.

The $S_1 \leftarrow S_0$ spectra of the different measured 2PY·fluorobenzenes break off at ∼780 cm^{-1} above their respective origins. In comparison to the spectrum of 2PY monomer, this corresponds to an extension of the spectrum by ∼60.[27,28] We have observed even more pronounced extensions of the $S_1 \leftarrow S_0$ spectra for strongly H-bonded dimers such as 2PY−uracil and 2PY−thymine.[33] We propose that this behavior is due to an interaction of the S_1 $\pi\pi^*$ excited state of 2PY with a slightly higher lying dark state that leads to rapid deactivation of the S_1 $\pi\pi^*$ state. As will be discussed below, hydrogen bond formation moves the S_1 $\pi\pi^*$ state to higher energy, corresponding to a spectral blue shift. It follows that the dark acceptor state is moved to even higher energies by H-bond formation.

D. Fluorescence Spectra and Intermolecular Vibrations in the S_0 State. In contrast to the $S_1 \leftarrow S_0$ spectra, which exhibit both inter- *and* intramolecular vibrational bands in the range 45−300 cm^{-1}, the low-wavenumber regions of the $S_1 \rightarrow S_0$ fluorescence spectra exhibit only intermolecular vibrational bands; the intramolecular $2\nu_1''$ or $2\nu_2''$ bands are not observed in emission. Such a lack of mirror symmetry is expected for emission from a quasiplanar vibrationless S_1 state to fully planar S_0 ground-state vibrational levels. Indeed, the bands at ∼455, ∼542, and ∼608 cm^{-1} can all be assigned to the in-plane totally symmetric intramolecular vibrations ν_4'', ν_5'', and ν_6'', respectively.

The fluorescence spectra of the seven complexes over the 0−130 cm^{-1} range are shown in Figures 4 and 5. We first discuss Figure 5: The spectrum of 2PY·1,3,5-FB clearly shows a strong σ'' band at ∼80 cm^{-1} and slightly weaker χ'' and ω'' bands at ∼40 cm^{-1}. A weak band on the low-wavenumber side of σ'' is tentatively assigned as the $2\theta''$ overtone or as the $\theta'' + \delta''$ combination. The σ'' band at ∼80 cm^{-1} and a slightly weaker ω'' band at ∼40 cm^{-1} are observed for 2PY·1,2,3-FB (Figure 5e) and for the tetrafluorobenzene complexes 2PY·1,2,3,4-FB and 2PY·1,2,4,5-tetrafluorobenzene (Figure 5f and g, respectively). The χ'' excitation is weaker in the 2PY·1,2,3-FB spectrum and cannot be observed in the fluorescence spectra of the two 2PY·tetrafluorobenzene complexes. Returning to the

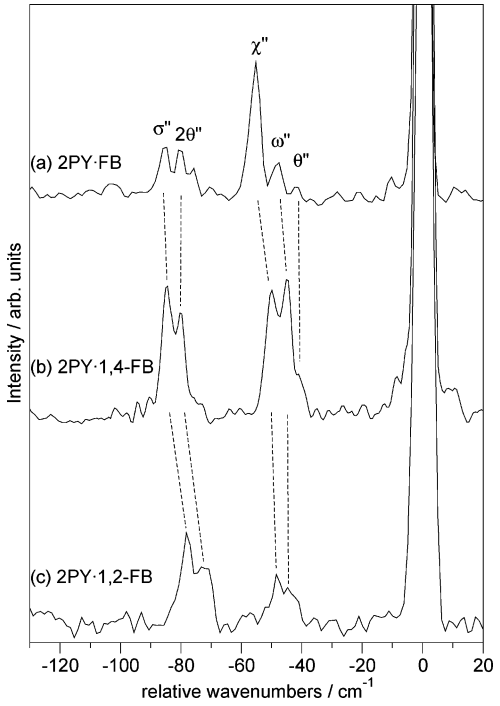

Figure 4. Low-wavenumber regions of the fluorescence emission spectra of (a) 2-pyridone·fluorobenzene, (b) 2-pyridone·1,4-difluorobenzene, and (c) 2-pyridone·1,2-difluorobenzene.

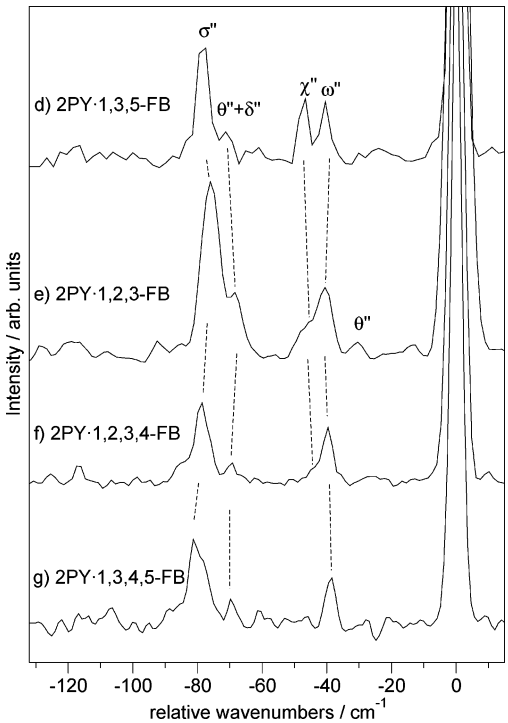

Figure 5. Low-wavenumber regions of the fluorescence spectra of (d) 2PY·1,3,5-trifluorobenzene, (e) 2PY·1,2,3-trifluorobenzene, (f) 2PY·1,2,3,4-tetrafluorobenzene, and (g) 2PY·1,2,4,5-tetrafluorobenzene.

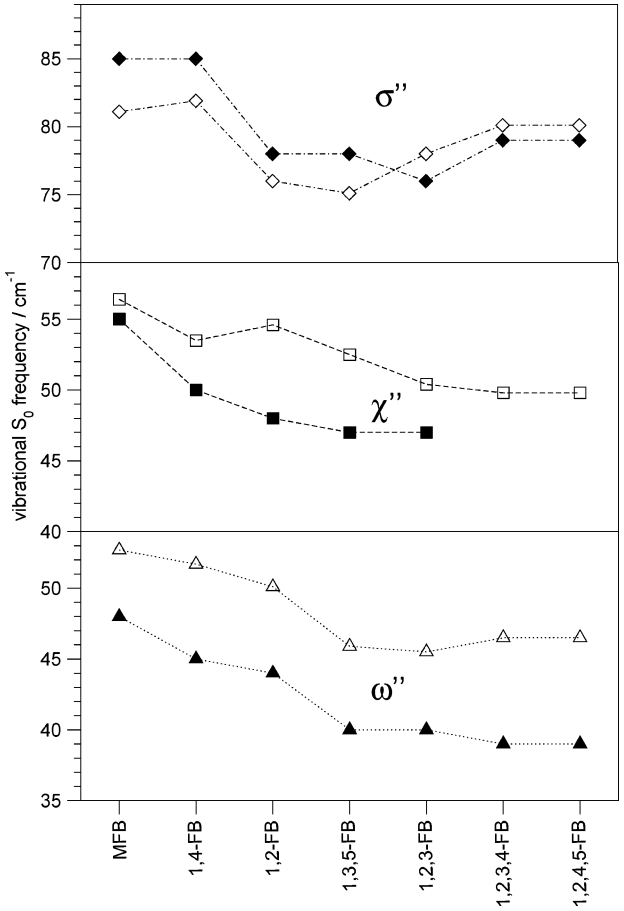

Figure 6. Comparison of B3LYP/6-311++G(d,p) calculated in-plane intermolecular S_0 state wavenumbers to experimental wavenumbers from fluorescence spectra. Filled symbols correspond to measured and empty symbols to calculated values.

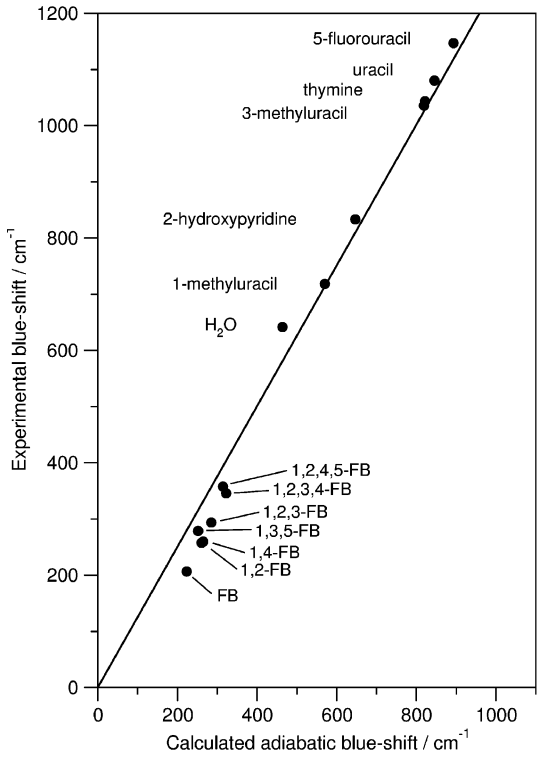

Figure 7. Experimental spectral blue shifts vs CIS/6-31G(d,p) calculated adiabatic spectral shifts. The observed/calculated shifts of the 2-pyridone·fluorobenzene complexes are combined with those of the complexes of 2-pyridone with 5-fluorouracil, uracil, thymine, 3-methyluracil, 2-hydroxypyridine, and 1-methyluracil (from ref 21), and with H_2O (from ref 19).

2PY·mono- and difluorobenzene spectra in Figure 4, we note that the χ'' shearing excitation is dominant for 2PY·FB and is also strong for 2PY·1,2-FB and 2PY·1,4-FB. The ω'' and σ'' bands are weaker but are clearly observed.

Comparing the seven 2PY·fluorobenzene fluorescence spectra, one sees that the Franck−Condon factor of the χ'' excitation is strongest for the 2PY·FB complex, undergoing a systematic decrease with increasing degree of fluorination. Practically the same decrease is observed in the $S_1 \leftarrow S_0$ R2PI spectra discussed in section III.B above and shown in Figure 2.

In Figure 6, we compare the B3LYP/6-311++G(d,p) calculated ground-state harmonic wavenumbers to the experimental values. As for the excited-state wavenumbers, the calculated ω'' and χ'' wavenumbers are predicted slightly too high. The calculated σ'' wavenumbers are very close to experiment, being within $\pm 1-3$ cm^{-1} of the measured values.

IV. Discussion

The intermolecular S_1 and S_0 state vibrational wavenumbers observed and discussed above provide strong evidence that the 2-pyridone·fluorobenzene complexes form hydrogen-bonded dimers. In both the ground and excited states, we observe three vibrational modes, as would be expected for planar or near-planar hydrogen-bonded geometries. Also, their wavenumbers are in near-quantitative agreement with the in-plane opening, shear, and stretching mode wavenumbers calculated for the S_0 and S_1 states. If the dimers were in fact π-stacked, we would expect to observe intermolecular vibrations with very low wavenumbers that correspond to tilting or twisting modes, in contrast to observation.

Further proof for hydrogen-bonded geometries comes from the observed spectral shifts. The electronic spectral shift $\delta\nu$ reflects the difference of the excited- and ground-state hydrogen bond dissociation energies, $D_0(S_1)$ and $D_0(S_0)$. Since the spectral shifts observed upon complexation are always to the blue (higher wavenumber), it follows that the H-bond strengths decrease upon electronic excitation. Spectral blue shifts have already been observed for a large number of singly and doubly hydrogen bonded complexes of 2-pyridone with H_2O,[19] NH_3,[20] 2-hydroxypyridine,[34] 2-aminopyridine,[35] uracil,[33] thymine,[33] 5-fluorouracil,[33] 1-methyl- and 3-methyluracil,[22] and 2-pyridone.[36−38] Although this correlation holds for all hydrogen-bonded complexes of 2-pyridone, we note that this chromophore behaves rather specially. Blue-shifted electronic spectra are *not* per se diagnostic for hydrogen-bonded complexes; in fact, there are many good examples in the literature of blue-shifted X−H···π bound complexes.[39,40]

In Figure 7, we compare the observed spectral shifts to the calculated adiabatic spectral shifts. For the latter, the S_0 state structures were optimized by RHF/6-31G(d,p), and the S_1 state structures by CIS/6-31G(d,p) calculations. The calculated shifts are given relative to that of bare 2-pyridone calculated with the same methods. Figure 7 also includes the observed and calculated spectral shifts for the other seven 2PY·fluorobenzene complexes discussed here. Their shifts clearly fall close to the correlation line established for the strongly H-bonded complexes, providing independent evidence for hydrogen bonding in the 2PY·fluorobenzene dimers with one to four fluorine atoms.

Furthermore, we have observed the R2PI spectra of *trimer* species consisting of a fluorobenzene moiety that is stacked on

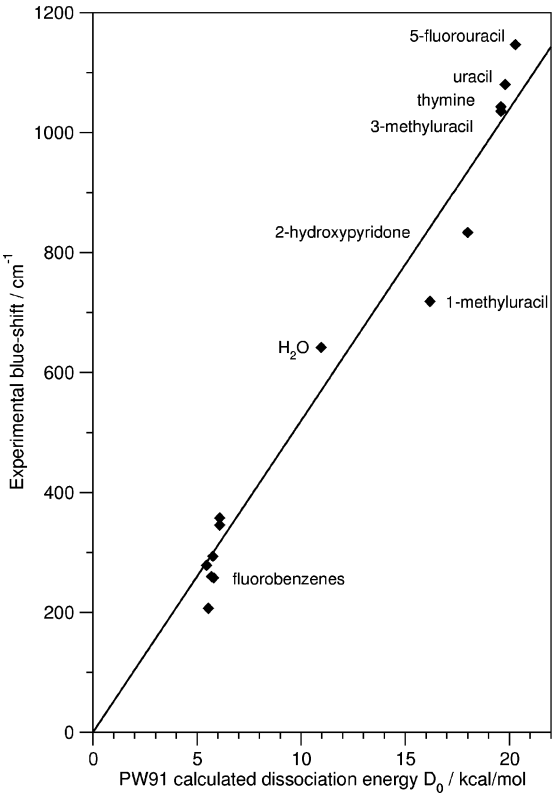

Figure 8. Experimental spectral blue shifts vs PW91/6-311++G(d,p) calculated ground-state dissociation energies $D_0(S_0)$, for the same hydrogen-bonded 2-pyridone complexes as in Figure 7.

the $(2PY)_2$ self-dimer. These spectra are strongly broadened compared to the spectrum of $(2PY)_2$[36−38] and of the hydrogen bonded dimers discussed here. While the absence of such broad spectra characteristic of π-stacked species for the 2PY·fluorobenzene complexes does not completely disprove the existence of π-stacked dimers, they must be $>10\times$ weaker than the spectra observed. The clear dominance of H-bonded dimer geometries is highly significant in view of the results from the DNA oligomer[1−10] and crystal studies and implies that fluorination cannot simply be equated with absence of H-bonding.

Since Figure 7 shows that the spectral shift correlates very well with the *difference* of the dissociation energies, $D_0(S_0) - D_0(S_1)$, one might expect the spectral shifts to correlate with the dissociation energy itself. In Figure 8, we plot the observed spectral shifts $\delta\nu$ versus the PW91 calculated ground-state dissociation energies $D_0(S_0)$. In the limit of no interaction, $\delta\nu$ must be 0, which is an additional condition for the regression line drawn in Figure 8. The spectral shift is indeed seen to correlate well with $D_0(S_0)$. The decrease of dissociation energy upon electronic excitation is roughly 13% of the ground-state dissociation energy.

V. Conclusions

Supersonically cooled complexes of the nucleobase mimic 2-pyridone, and seven different fluorobenzenes (1-FB, 1,2-FB, 1,4-FB, 1,3,5-FB, 1,2,3-FB, 1,2,4,5-FB, 1,2,3,4-FB) have been spectroscopically characterized. Their $S_1 \leftarrow S_0$ resonant two-photon ionization and $S_1 \rightarrow S_0$ fluorescence spectra are characteristic for hydrogen-bonded geometries. This implies that the hydrogen bond interactions in these dimers have considerable strength. This is in strong contrast to room-temperature studies on closely related complexes of the thymidine mimic 2,4-difluorotoluene.[41,42]

On the other hand, we have not been able to observe any spectroscopic features characteristic of π-stacked complexes. This implies that the hydrogen bond interactions are stronger than the π-stacking interactions in these 2PY·fluorobenzene complexes. In a companion paper, we have calculated binding and dissociation energies of the same complexes using the resolution of identity MP2 method, large basis sets, and complete basis set (CBS) extrapolation techniques.[24] The extrapolated binding energies for the C−H···O=C and N−H···F−C hydrogen-bonded dimers are $-D_{e,CBS} = 6.5-7$ kcal/mol, increasing by <10% between mono- and tetrafluorobenzene. The respective dissociation energies D_0, which include zero-point vibrational effects, are ~0.5 kcal/mol smaller and represent upper limits to the stacking energies of these complexes.

The $S_1 \leftrightarrow S_0$ resonant two-photon ionization spectra fluorescence spectra show vibronic bands that are characteristic for the in-plane opening, shear, and stretching vibrations between the 2-pyridone and fluorobenzene moieties. The intermolecular stretching frequencies decrease by 5−10% upon $S_1 \leftarrow S_0$ electronic excitation, indicating a weakening of the hydrogen bonds to the 2-pyridone moiety. The decrease of hydrogen bond strength also leads to spectral blue shifts $\delta\nu$ of the $S_1 \leftarrow S_0$ electronic origin. The observed and calculated spectral blue shifts of 15 different hydrogen-bonded 2PY complexes observed so far are in excellent agreement over a range from $\delta\nu \approx +240$ cm^{-1} for 2-pyridone·fluorobenzene up to $\delta\nu \approx +1000$ cm^{-1} for the 2-pyridone·uracil.[22,33]

More importantly, the experimentally observed decreases of the H-bond dissociation energy correlate very well with the hydrogen-bond ground-state dissociation energies over a range from 3 to 10 kcal/mol per hydrogen bond. This correlation establishes a gas-phase experimental scale for measuring H-bond energies to the nucleobase mimic 2-pyridone.

Acknowledgment. This work was supported by the Schweiz.Nationalfonds (project 200020-105490).

References and Notes

(1) Moran, S.; Ren, R. X.-F.; Kool, E. T. *Proc. Natl. Acad. Sci. U.S.A.* **1997**, *94*, 10506.
(2) Goodman, M. F. *Proc. Natl. Acad. Sci. U.S.A.* **1997**, *94*, 10493.
(3) Kool, E. T.; Morales, J. C.; Guckian, K. M. *Angew. Chem., Int. Ed.* **2000**, *39*, 990.
(4) Pasch, J.; Engels, J. W. *Helv. Chim. Acta* **2000**, *83*, 1791.
(5) Kool, E. T. *Annu. Rev. Biophys. Biomol. Struct.* **2001**, *30*, 1.
(6) Mathis, G.; Hunziker, J. *Angew. Chem., Int. Ed.* **2002**, *41*, 3203.
(7) Kool, E. T. *Annu. Rev. Biophys.* **2002**, *71*, 191.
(8) Lai, J. S.; Qu, J.; Kool, E. T. *Angew. Chem., Int. Ed.* **2003**, *42*, 5973.
(9) Lai, J. S.; Kool, E. T. *J. Am. Chem. Soc.* **2004**, *126*, 3040.
(10) Henry, A. A.; Olsen, A. G.; Matsuda, S.; Yu, C.; Geierstanger, B. H.; Romesberg, F. E. *J. Am. Chem. Soc.* **2004**, *126*, 6923.
(11) Shimoni, L.; Glusker, J. P. *Struct. Chem.* **1994**, *5*, 383.
(12) Thalladi, V. R.; Weiss, H.-C.; Bläser, D.; Boese, R.; Nangia, A.; Desiraju, G. R. *J. Am. Chem. Soc.* **1998**, *120*, 8702.
(13) Dunitz, J. D. *ChemBioChem* **2004**, *5*, 614.
(14) Ohtsuki, T.; Kimoto, M.; Ishikawa, M.; Mitsui, T.; Hirao, I.; Yokoyama, S. *Proc. Natl. Acad. Sci. U.S.A.* **2001**, *98*, 4922.
(15) Hirao, I.; Ohtsuki, T.; Fujiwara, T.; Mitsui, T.; Yokogawa, T.; Okuni, T.; Nakayama, H.; Takio, K.; Yabuki, T.; Kigawa, T.; Kodama, K.; Nishikawa, K.; Yokoyama, S. *Nat. Biotechnol.* **2002**, *20*, 177.
(16) Kimoto, M.; Endo, M.; Mitsui, T.; Okuni, T.; Hirao, I.; Yokoyama, S. *Chem. Biol.* **2003**, *11*, 47.
(17) Hirao, I.; Harada, Y.; Kimoto, M.; Mitsui, T.; Fujiwara, T.; Yokoyama, S. *Proc. Natl. Acad. Sci. U.S.A.* **2004**, *126*, 13298.
(18) Held, A.; Pratt, D. *J. Chem. Phys.* **1992**, *96*, 4869.
(19) Held, A.; Pratt, D. *J. Am. Chem. Soc.* **1993**, *115*, 9708.
(20) Held, A.; Pratt, D. *J. Am. Chem. Soc.* **1993**, *115*, 9718.
(21) Frey, J. A.; Müller, A.; Frey, H.-M.; Leutwyler, S. *J. Chem. Phys.* **2004**, *121*, 8237.
(22) Müller, A.; Frey, J. A.; Leutwyler, S. *J. Phys. Chem. A* **2005**, *109*, 5055.

(23) Frey, J. A.; Leutwyler, S. *Chimia* **2005**, *59*, 511.
(24) Frey, J. A.; Leist, R.; Leutwyler, S. *J. Phys. Chem. A* **2006**, *110*, 4188.
(25) Frisch, M. J.; Trucks, G. W.; Schlegel, H. B.; Scuseria, G. E.; Robb, M. A.; Cheeseman, J. R.; Montgomery, J. A., Jr.; Vreven, T.; Kudin, K. N.; Burant, J. C.; Millam, J. M.; Iyengar, S. S.; Tomasi, J.; Barone, V.; Mennucci, B.; Cossi, M.; Scalmani, G.; Rega, N.; Petersson, G. A.; Nakatsuji, H.; Hada, M.; Ehara, M.; Toyota, K.; Fukuda, R.; Hasegawa, J.; Ishida, M.; Nakajima, T.; Honda, Y.; Kitao, O.; Nakai, H.; Klene, M.; Li, X.; Knox, J. E.; Hratchian, H. P.; Cross, J. B.; Bakken, V.; Adamo, C.; Jaramillo, J.; Gomperts, R.; Stratmann, R. E.; Yazyev, O.; Austin, A. J.; Cammi, R.; Pomelli, C.; Ochterski, J. W.; Ayala, P. Y.; Morokuma, K.; Voth, G. A.; Salvador, P.; Dannenberg, J. J.; Zakrzewski, V. G.; Dapprich, S.; Daniels, A. D.; Strain, M. C.; Farkas, O.; Malick, D. K.; Rabuck, A. D.; Raghavachari, K.; Foresman, J. B.; Ortiz, J. V.; Cui, Q.; Baboul, A. G.; Clifford, S.; Cioslowski, J.; Stefanov, B. B.; Liu, G.; Liashenko, A.; Piskorz, P.; Komaromi, I.; Martin, R. L.; Fox, D. J.; Keith, T.; Al-Laham, M. A.; Peng, C. Y.; Nanayakkara, A.; Challacombe, M.; Gill, P. M. W.; Johnson, B.; Chen, W.; Wong, M. W.; Gonzalez, C.; Pople, J. A. *Gaussian 03*, revision A.01; Gaussian, Inc.: Pittsburgh, PA, 2003.
(26) Müller, A.; Losada, M.; Leutwyler, S. *J. Phys. Chem. A* **2004**, *108*, 157.
(27) Nimlos, M. R.; Kelley, D. F.; Bernstein, E. R. *J. Phys. Chem.* **1989**, *93*, 643.
(28) Ozeki, H.; Cockett, M. C. R.; Okuyama, K.; Takahashi, M.; Kimura, K. *J. Phys. Chem.* **1995**, *99*, 8608.
(29) Held, A.; Champagne, B. B.; Pratt, D. *J. Chem. Phys.* **1991**, *95*, 8732.
(30) Matsuda, Y.; Ebata, T.; Mikami, N. *J. Chem. Phys.* **1999**, *110*, 8397.
(31) Matsuda, Y.; Ebata, T.; Mikami, N. *J. Chem. Phys.* **2000**, *113*, 573.
(32) Frey, J. A.; Leist, R.; Leutwyler, S. Manuscript in preparation.
(33) Müller, A.; Leutwyler, S. *J. Phys. Chem. A* **2004**, *108*, 6156.
(34) Müller, A.; Talbot, F.; Leutwyler, S. *J. Chem. Phys.* **2001**, *115*, 5192.
(35) Müller, A.; Talbot, F.; Leutwyler, S. *J. Am. Chem. Soc.* **2002**, *124*, 14486.
(36) Held, A.; Pratt, D. *J. Am. Chem. Soc.* **1990**, *112*, 8629.
(37) Müller, A.; Talbot, F.; Leutwyler, S. *J. Chem. Phys.* **2000**, *112*, 3717.
(38) Müller, A.; Talbot, F.; Leutwyler, S. *J. Chem. Phys.* **2002**, *116*, 2836.
(39) Gotch, A. J.; Zwier, T. S. *J. Chem. Phys.* **1990**, *93*, 6977.
(40) Gotch, A.; Garrett, A.; Severance, D.; Zwier, T. *J. Chem. Phys.* **1991**, *96*, 3388.
(41) Schmidt, K. S.; Sigel, R. K. O.; Filippov, D. V.; van der Marel, G. A.; Lippert, B.; Reedijk, J. *New J. Chem.* **2000**, *24*, 195.
(42) Sherer, E. C.; Bono, S. J.; Shields, G. C. *J. Phys. Chem. B* **2001**, *105*, 8445.